



Research Article

n-Graphene/p-Silicon-based Schottky junction solar cell, with very high power conversion efficiency

A. J. Wirth-Lima¹  · P. P. Alves-Sousa² · W. Bezerra-Fraga^{1,2}

Received: 24 October 2019 / Accepted: 15 January 2020 / Published online: 21 January 2020
© Springer Nature Switzerland AG 2020

Abstract

We are presenting a solar cell consisting of electron-doped graphene (n-G)/holes-doped silicon (p-Si) Schottky junction, which provides a very high power conversion efficiency (PCE). The high PCE of our solar cell is caused by its high Schottky barrier height, which gives a very low value for the saturated reverse current (I_0), and consequently, occurs a very low value of the current flowing through the forward-biased Schottky junction (value tending to zero). Therefore, as all photogenerated current goes to the external circuit, the solar cell PCE, we are presenting is very high, which exceeds the Shockley–Quiesser limit. It is noteworthy that the n-G/p-Si solar cells with resistance series $R_s = 17.52 \Omega$, and $R_s = 10.00 \Omega$ presented PCE values $\approx 22.55\%$, and $\approx 39.51\%$, respectively. Since there is no current going through the Schottky junction, that n-G/p-Si solar cell operates similarly to an electrochemical generator. To get the characteristic parameters of our solar cell, we used an analytical/numerical methodology.

Keywords Doped graphene · Power conversion efficiency · Schottky junction · Schottky barrier height · Solar cell

1 Introduction

Solar cells can be classified into first, second, and third generation. The first generation of solar cells consists of conventional solar cells, composed of P–N junctions of crystalline silicon (c-Si) wafers. The silicon used in these solar cells can be monocrystalline (Mono-c Si) or polycrystalline (Poly-c Si). There are also solar cells made of amorphous silicon (a-Si), but in this case, these solar cells may belong to the first or second generation.

Mono-c Si solar cells are obtained from a single Si crystal having a single orientation in their molecular structure and providing higher photovoltaic conversion efficiency (up to 26% [1]). On the other hand, Poly-c Si cells are made from several different Si crystals, i.e., they have heterogeneity in their internal molecular orientation (conversion efficiency up to 21% [1]).

The second generation of solar cells are known as thin-film solar cells (TFSCs), due to their layers of only a few micrometers thick. These solar cells consist of cadmium telluride (CdTe) and copper indium gallium selenide (CIGS) thin films (among others) and currently may have up to 12% conversion efficiency [1]. Although TFSCs have lower conversion efficiency, larger dimensions, and shorter longevity than c-Si solar cells, they are cheaper.

The third generation of solar cells, which may contain graphene, and/or other 2D materials, is also based on thin film but is still in the research and development stage. Examples of the third generation of solar cells are dye-sensitized solar cells (DSSCs) [2], organic solar cells (OSCs), or plastic solar cells, Perovskite solar cells [3], plasmonic solar cells, quantum dot solar cells, Schottky junction graphene/silicon solar cells [4–9], and graphene/other 2D materials hybrid solar cells.

✉ A. J. Wirth-Lima, awljeng@gmail.com | ¹Department of Physics, Federal Institute of Education, Science and Technology of Ceará, Campus Sobral, Fortaleza, Ceará, Brazil. ²Postgraduate Program in Electrical Engineering and Computing, Federal University of Ceará (U.F.C.), Sobral, Ceará, Brazil.



Indeed graphene may be used in almost all cell types mentioned above. It is noteworthy that Indium Tin Oxide (ITO) is used with a non-conductive glass layer as a transparent electrode. However, as ITO is rare and brittle, the solar cells utilizing this material are expensive and unstable. Hence, as graphene has excellent conductivity, high transparency, low reflection, low electrical resistance, and cost-effective, it can replace ITO as a high-efficient transparent electrode for solar cells. Moreover, graphene has a bias tunable Schottky barrier height, via chemical or electrical doping, for example, enabling the replacement of the metal by graphene (with many advantages) in solar cells constituted by Schottky junction.

The power conversion efficiency (PCE) for graphene-based solar cells rapidly passed from the initial value of ≈ 1.5 to $\approx 15\%$ [4–9], by controlling the number of graphene layers, addition of antireflection film, use of modified graphene films and silicon columns forming the Schottky junction, removing of PMMA residues left in the graphene during its transfer process, as much as possible, and controlling of the graphene work function by the insertion of chemical doping. However, the large loss of the photogenerated due to the current that crosses the Schottky junction (I_d), and does not contribute to external current, was not considered. On the other hand, in the solar cell we are presenting, there is practically no I_d current so that all photogenerated current goes to the external circuit, and the power conversion efficiency (PCE) of this solar cell is still enormously increased. This is possible by the use of more appropriate values of the Schottky junction parameters. Note that the increase of the Schottky barrier height (SBH) can be obtained by changing the graphene work function. Hence, as a higher SBH causes a great decrease of the saturated reverse current (I_0), and consequently, for a very small I_0 (as it has been reached), the current that crosses the diode (for the voltage range of this type of solar cell) is very small so that it can be neglected.

Currently, the maximum SBH for Schottky junctions consisting of p-doped graphene/n-doped silicon (p-G/n-Si) is ≈ 0.8 eV. On the other hand, an n-doped graphene/p-doped silicon (n-G/p-Si) Schottky junction can be obtained from graphene doped with metallic dopants so that its SBH has a very higher value (≈ 2.94 eV). Therefore, as the n-G/p-Si Schottky junction has an SBH and built-in potential (Φ_{bi}) with very high values, solar cells constituted by this referred Schottky junction have a high power conversion efficiency.

We are presenting a solar cell based on the n-G/psi Schottky junction, working similar to an electrochemical generator that has a very high energy conversion efficiency, which may exceed the Shockley–Quiesser limit.

This manuscript has three more sections. In Sect. 2, we detail the starting point for the determination of all parameters of the n-G/p-Si solar cell we are presenting. In Sect. 3, we present details of that referred n-G/p-Si solar cell. Section 4 is devoted to the conclusions regarding what we are presenting.

2 p-Graphene/n-silicon and n-graphene/p-silicon solar cells (start point)

In Fig. 1, we are presenting a simple but efficient way to determine the operation of a graphene/silicon Schottky junction solar cell.

As it is shown in the upper left-hand part of this Figure, the generated charges (due to the absorption) are separated by the built-in field so that in the p-graphene (p-G)/n-silicon (n-Si) solar cells, holes are routed to the graphene, and electrons are moved to the silicon. However, these charges provide a forward bias polarization of the Schottky junction so that part of the photogenerated charges cause an internal current through the forward bias Schottky junction (diode current— I_d). Hence, only a part of the generated charges contributes to the external current (I , electrons current, first quadrant).

Since the value of the shunt resistance (R_{sh}) related to this type of solar cell is very high (up to 45 M Ω) [6], we can neglect the leakage current I_{sh} . Therefore,

$$I = I_{ph} - I_d \rightarrow I_d = I_{ph} - I \quad (1)$$

where $I_{ph} \approx I_{sc}$ represent the photogenerated current and the short-circuit current, respectively.

In the upper right-hand part of Fig. 1, we are showing the behavior of this solar cell operating with an external short circuit. Note that in this case, we can consider that the voltage applied at the Schottky junction is zero, which causes the current I_d not to exist. Hence, in this case, all the photogenerated charges contribute to the external current (whose value is I_{sc} —short circuit current). On the other hand, in the lower left-hand part of Fig. 1, it is shown the open circuit operation, where we can observe that the voltage applied at the Schottky junction has the maximum value (V_{oc} —open circuit voltage). Therefore in this situation, the current through the diode has maximum value (I_{sc}). We can see the schematic representation of the electric circuit of this type of solar cell in the lower right-hand part of Fig. 1.

Although the process of cleaning, transfer, and doping of graphene, has been greatly improved, the power conversion efficiency (PCE) of this type of solar cell is still low. This mainly occurs, because the electric current flowing through the forward-biased diode is relatively high,

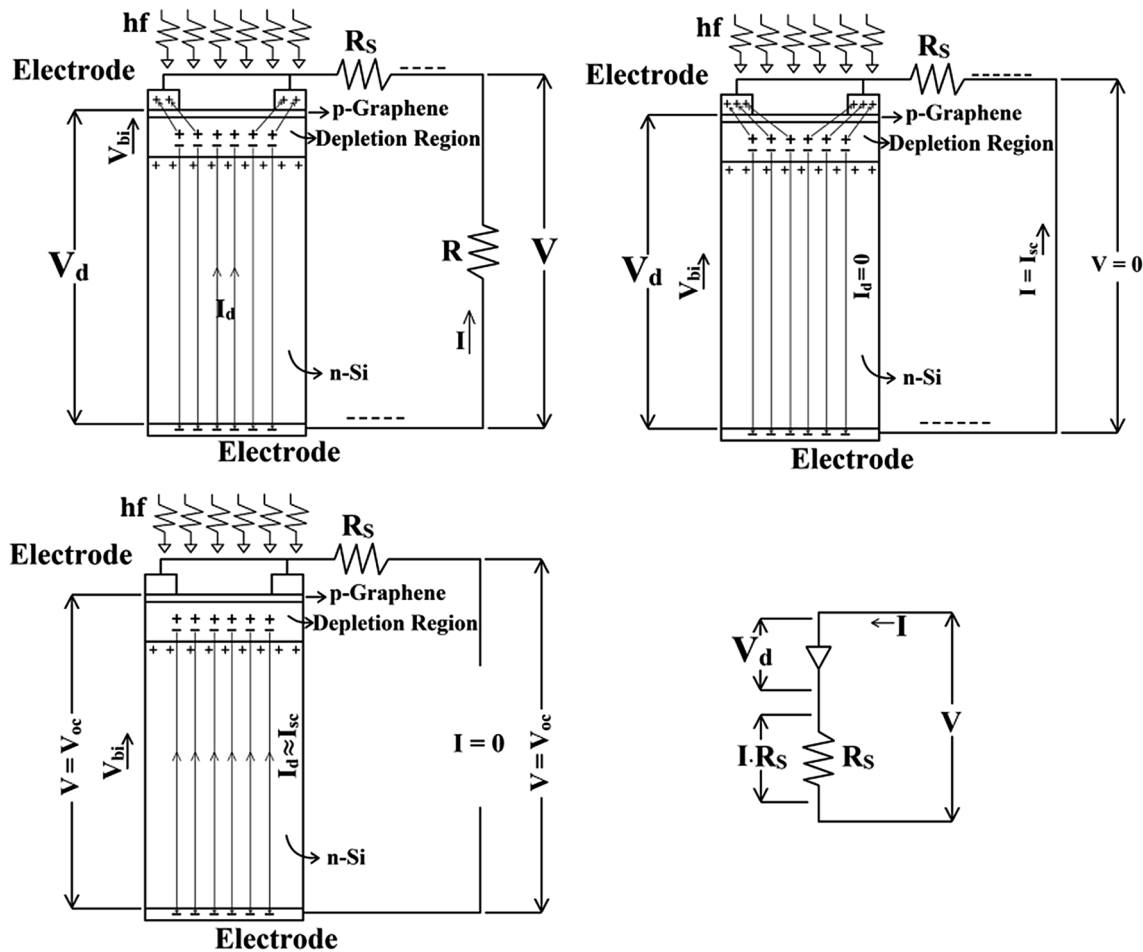


Fig. 1 Schematic representation of the operation of a Schottky junction-based p-G/n-Si solar cell. Upper left: external circuit with resistance R . Upper right: short circuit. Bottom left: open circuit. Bottom right: electrical circuit

and does not contribute to the external circuit current. In other words, according to Eq. 1, the value of the external current decreases as a function of the current that crosses the forward bias diode.

To facilitate the presentation of the n-G/p-Si solar cell we are presenting, we will first detail a p-G/n-Si solar cell.

Let us assume the data presented for a given p-G/n-Si solar cell [1]: (V, I) measured data, open circuit voltage $V_{oc} \approx 0.548$ V, and short circuit current $I_{sc} \approx 7.819$ mA (solar cell exposed to the environment). We got the (V, I) curve (and (V, I_d) curve referring to the solar cell mentioned above, using several points of the (V, I) curve obtained via simulations, according to the which is shown at the top of Fig. 2 (solid and dashed line, respectively; y-axis located on the left side).

In this same Figure, we are showing the (V, P) curve (dashed and dotted line; y-axis located on the right side). The value of the maximum power is $P_{max} \approx 0.00222$ W, the fill factor value is $FF = V_{max} * I_{max} / V_{oc} * I_{sc} \approx 51.69\%$, and the PCE value is $\approx 11.66\%$.

We determined the PCE value using the following Equation:

$$\eta = \frac{P_m}{AG} \tag{2}$$

where P_m is the maximum power supplied by the solar cell and $G = 1000$ W/m² is the value of the solar radiation power under the AM1.5 conditions.

There are several analytical methods for determining the parameters of a solar cell from the data obtained through simulations [10–14]. However, to show the behavior of the p-G/n-Si solar cell, we used the data obtained in the above-mentioned simulations.

At the bottom of Fig. 2, we are showing the graph (I, V) . Note that the voltage at the external circuit varies according to the value of the external current intensity. Moreover, the voltage value in the external circuit decays approximately linearly as a function of the current rise

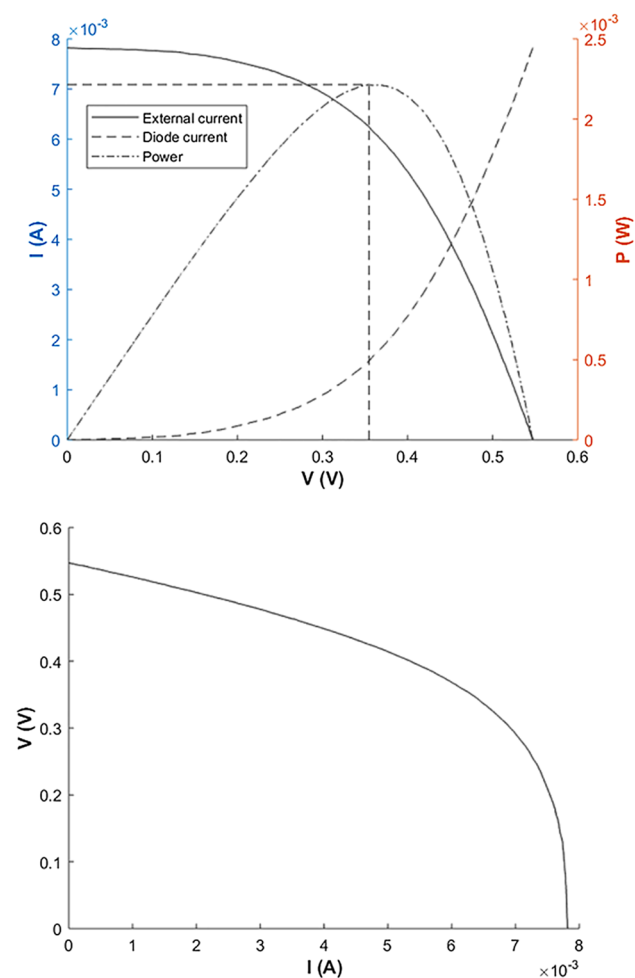


Fig. 2 Top: (V, I) curve (V, Id) curve, (y axis located on the left side), and (V, P) curve (y axis located on the right side), referring to the p-graphene/n-silicon solar cell mentioned above. Bottom: (I, V) curve

up to 5 mA. From this value, it decays exponentially and has a null value in the short-circuit condition.

Due to its imperfections and the charged impurities located on the substrate, real graphene has non-zero intrinsic charge density [15, 16]. Hence, its Fermi level is not located at the Dirac point. In a research carried out it has been demonstrated that the dry transfer of graphene films to the standardized substrate (SiO₂/Si), as well as the subsequent cleaning through modified Radio Corporation of America (RCA) procedure, provides production of devices composed of graphene with low Dirac voltage ($V_D < 4.5$ V) [17]. In a research where the quantum capacitance of graphene has been measured (single and bilayer samples) as a function of gate potential, it has been found the residual graphene carrier concentration $n^* \approx 8 \times 10^{11} \text{ cm}^{-2}$ [18]. Note that the Dirac voltage value depends on the efficiency of the graphene manufacturing and transport process.

Changes in graphene work function values, due to the effects of doping of graphene with arsenic and with phosphorus were elaborated through a Metal–Organic Chemical Vapor Deposition (MOCVD) reactor. Therefore, using the chemical doping of graphene, with phosphorus and arsenic, its work function increases from 4.5 eV (undoped graphene) to 4.7 eV and 4.8 eV, for phosphorus and arsenic, respectively, and as a consequence, there is an increase of the potential barrier [19]. However, this value of Φ_B is still very low, so that the current through the forward-biased diode is very high.

Taking into consideration that in the n-G/p-Si solar cell the value of Φ_B is relatively high (this subject will be detailed later), for comparison, we will determine the potential barrier value for a Schottky p-G/n-Si, with graphene having work function $\Phi_G = 4.8$ eV.

It is well known that for a Schottky junction, the Fermi level of the n-silicon substrate (after the depletion zone) is shifted upwards, according to the following Equation:

$$\Delta E_F = k_B T \ln \left(\frac{N}{n_i} \right). \tag{3}$$

As the charge doping density of n-Si is $N = 10^{17} \text{ cm}^{-3}$, the silicon intrinsic density of charge carriers $n_i \approx 1.45 \times 10^{10} \text{ cm}^{-3}$ (value found from the effective densities of states of electrons and holes in the conduction and valence bands, respectively, of a silicon intrinsic semiconductor), the value of the displacement of the silicon Fermi level is $\Delta E_F = 0.407$ eV (upward). Therefore, in this case, the energy level of the n-silicon conduction band is given by $E_c = E_g/2 - \Delta E_F \approx 0.153$ eV ($E_g = 1.12$ eV is the silicon bandgap value) above the Fermi level. Hence, considering that the value of the electron affinity of silicon is $\chi = 4.05$ eV, and $\Phi_G = 4.80$ eV we determined, analytically, the values of the Schottky barrier height ($\Phi_B = \Phi_G - \chi \approx 0.75$ eV) and of the built-in barrier height ($\Phi_{bi} = \Phi_G - \chi - E_c \approx 0.597$ eV) referring to this p-G/n-Si Schottky junction, as shown in Fig. 3 (without illumination).

It is noteworthy that the Φ_B value determined by this methodology is very close to the actual value since only the influences concerning the image force barrier lowering and charge traps on the interface and native oxide are not considered. However, the image force barrier lowering produces only small deviations from the value of Φ_B [20]. Furthermore, by using an optimized graphene transfer process, it is possible to obtain an interface with a small number of atomic defects. This procedure, together with actions that prevent the formation of silicon dioxide, provides the reduction of the charge traps so that we can neglect the influence of these charge traps [21]. It is noteworthy that the determination of

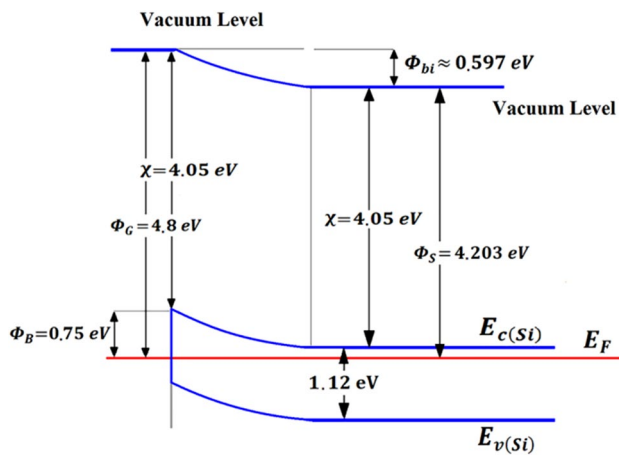


Fig. 3 p-G/n-Si Schottky junction energy band structure at thermodynamic equilibrium (without illumination)

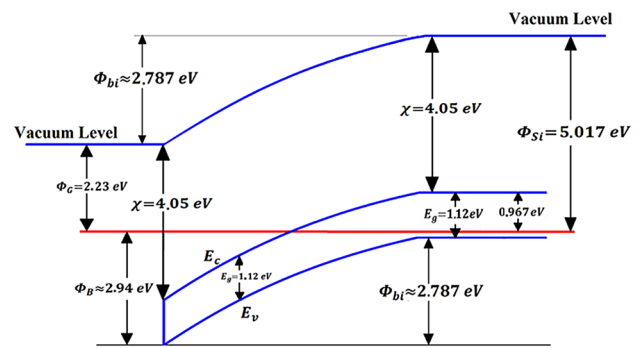


Fig. 4 n-G/p-Si Schottky junction energy band structure at thermodynamic equilibrium (without illumination)

the Schottky barrier height is the starting point for our n-G/p-Si solar cell.

From thermionic emission theory, the Equation that provides the current through the external circuit (I) in a Schottky junction solar cell as a function of the voltage (V) (in the load resistance) is given by:

$$I(T, V) = I_0 \left[e^{\frac{qV_d}{\eta k_B T}} - 1 \right] + \frac{V + R_s I}{R_{sh}} - I_{ph} \tag{4}$$

$$I_0(T) = AA^* T^2 e^{-\frac{q\Phi_B}{k_B T}}, \tag{5}$$

which can be solved numerically. We used MATLAB for the numerical resolution of all Equations presented in this manuscript.

It is worth mentioning that in Eqs. 3 and 4, I_0 is the saturated reverse current, V_d is the voltage at the Schottky junction, η the ideality factor, k_B the Boltzmann constant, T the ambient temperature, A the effective area of contact, and A^* the Richardson's constant.

Entering the value of Φ_B given above in Eq. 5 (considering $A = 0.19 \text{ cm}^2$), we determined the value of $I_0 = 4.822 \times 10^{-7} \text{ A}$, which is still very high.

It is important to state, that the greater the value of Φ_B , the lower the value of I_0 , and consequently, the lower is the I_d value. So we must choose a solar cell structure that gives a large value of Φ_B . Therefore, the doping of graphene is essential to increase the efficiency of this type of solar cell.

3 n-Graphene/p-silicon-based Schottky junction solar cell with very high PCE

According to we have mentioned earlier, larger SBH provides smaller saturated reverse current value, and consequently, smaller current crossing the Schottky junction operating as a forward-biased diode. From the energy band diagram, related to the solar cell to be designed, we can obtain the highest possible SBH, by choosing the more appropriated types of doping for graphene and silicon (n, or p).

n-doped graphene (n-G) can be obtained from metallic dopants so that its work function is reduced (for example, to 2.23 eV, using K-doped graphene [22, 23]). Therefore, an n-G/p-Si Schottky junction may have an SBH with a much higher value than a p-G/n-Si Schottky junction, as we can see in Fig. 4.

For the elaboration of Fig. 4, we used the same values related to charge doping density ($N = 10^{17} \text{ cm}^{-3}$), as well as intrinsic density of charge carriers ($n_i \approx 1.45 \times 10^{10} \text{ cm}^{-3}$), and electron affinity for the silicon used in the p-G/n-Si Schottky junction. As we can see, we determined analytically the values of the Schottky barrier height ($\Phi_B = E_g + \chi - \Phi_G \approx 2.94 \text{ eV}$), and of the built-in barrier height ($\Phi_{bi} = \Phi_B - E_v \approx 2.787 \text{ eV}$, where $E_v = E_g - E_c$ is the energy level of the p-silicon valence band), referring to the n-G/p-Si solar cell we are presenting.

It is noteworthy that we can use the following equation to determine the value of the variation of the Fermi level (or the chemical potential) of graphene, $\Delta\mu_g$ [24, 25]:

$$\Delta\mu_g = \Delta E_F = \hbar V_F \sqrt{n\pi}, \tag{6}$$

where \hbar is the Planck's reduced constant, V_F is the Fermi velocity for graphene (10^6 m/s), and n the charge carrier density. So, as the graphene Fermi level can be altered in several ways (for example, via chemical doping, or gate voltage), the graphene work function can also be changed,

and consequently, the graphene/semiconductor potential barrier can be altered too, according to what was mentioned previously.

On the other hand, due to the application of an external voltage, there is a variation of the density of electrons located in graphene (n_g) and holes in n-Si at a graphene/silicon Schottky junction. Note that the variation of the density of electrons in graphene is the same variation of the density of holes located in the n-semiconductor depletion region [26]. For forward voltage, the number of holes in the semiconductor depletion zone decreases, which leads to the decrease of electrons in the graphene. So, in this case, the Fermi level is shifted down. It is noteworthy that for reverse voltage (considered as $V < 0$), the number of holes in the depletion zone increases, resulting in the negative value of n_g , so that the Fermi level of the graphene is shifted upwards. Therefore, with the Schottky junction under illumination, the Fermi level of graphene is shifted downward (forward bias diode). However, due to the small values of the voltage in a solar cell, this displacement is very small and can be neglected.

By inserting the value of the SBH in Eq. 5, we determined the value of $I_0 \approx 7.84 \times 10^{-44}$ A. Hence, in this case, the current flowing through the forward-biased diode is very small, so that it can be neglected, according to what we show below.

In Fig. 5 we are showing the schematic representation of the n-G/p-Si solar cell we are presenting.

Since there is no current flowing through the Schottky junction, in this case, all the photogenerated charge is routed to the electrodes. Hence, in this type of solar cell, the external current is provided by the fixed voltage that occurs in the Schottky junction (electromotive force (ϵ)), which is given by $\epsilon = V + IR_s$, as we can see from Fig. 5.

To represent the behavior of the n-G/p-Si solar cell, we first consider the voltage at the Schottky junction referring to the p-G/n-Si solar cell, which is given by $V_d = V + IR_s$.

We obtained the R_s value (17.52Ω) through the methodology presented in Ref. [27], taking into account the range of values close to the final part of the (V, I_d) curve referring to the forward bias diode (p-G/n-Si solar cell). It is worth mentioning that the series resistance of this type of solar cells presented values between 9 and 12Ω , for a voltage range between 0.1 and 2.0 V [6].

The curves (I, V) and (I, V_d) are shown at the top of Fig. 6 (for $R_s = 17.52 \Omega$).

Note that the value of I_{sc} occurs for the minimum value of $V_d (\approx 0.137 \text{ V})$. Also, note in this Fig. 6, the graphical representation of the constant value of ϵ for the n-G/P-Si solar cell.

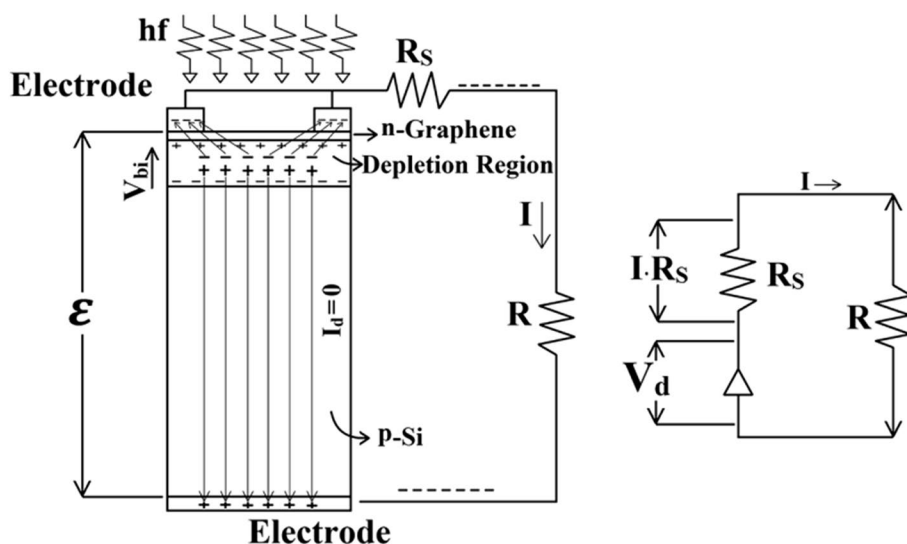
On the other hand, as in the n-G/P-Si solar cell, there is no current flowing through the forward bias diode, all the current goes to the external circuit so that this solar cell we are presenting operates similarly to an electrochemical generator. Note that in this case, this solar cell has an electromotive force $\epsilon = \max(V + IR_s) = V_{oc}$. Therefore, in this case, $I_{sc} = \epsilon/R_s \approx 0.0313 \text{ A}$.

For comparison, the (V, I) curves for n-G/p-Si (solid line) and p-G/n-Si (dashed line) solar cells are plotted at the bottom of Fig. 6. Note that the curve (V, I) for the solar cell n-G/p-Si is a straight line, just as it is in an electrochemical generator.

The graphs (V, P) for p-G/n-Si and n-G/p-Si with $R_s = 17.52 \Omega$, and $R_s = 10.00 \Omega$ solar cells are shown in Fig. 7.

We determined the value of the maximum power and PCE of the solar cells p-G/n-Si, and n-G/p-Si with $R_s = 17.52 \Omega$, and $R_s = 10.00 \Omega$ i.e., $P_{max} \approx 0.00222 \text{ W}$ ($V_{max} \approx 0.355 \text{ V}$, $I_{max} \approx 0.0063 \text{ A}$); $PCE \approx 11.66\%$ (these values have already been shown in Sect. 2), $P_{max} \approx 0.00429 \text{ W}$

Fig. 5 Schematic representation of the operation of a solar cell based on n-G/p-Si Schottky junction



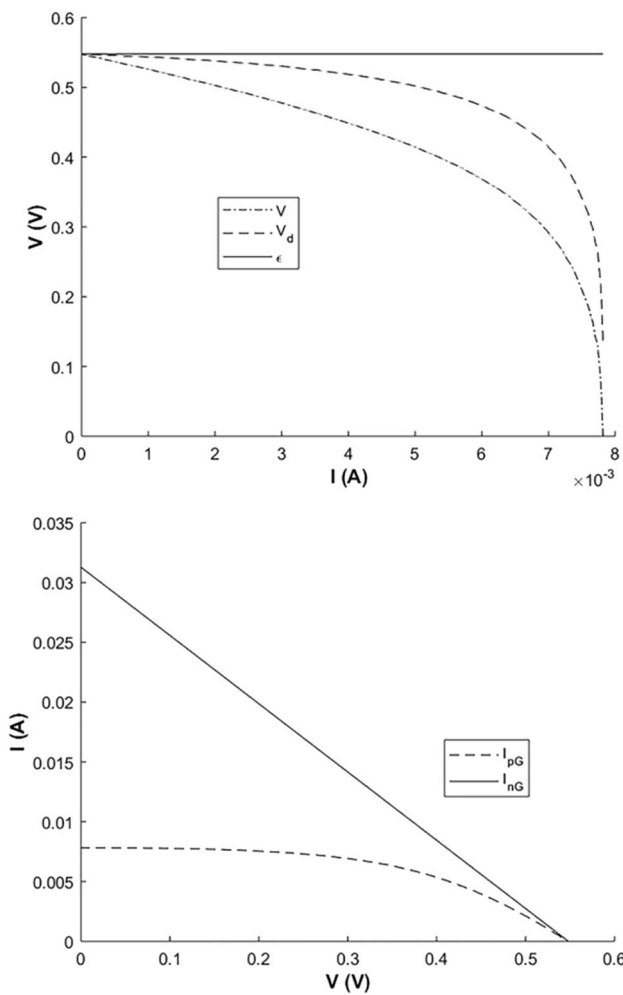


Fig. 6 Top: (I, V) , (I, V_d) , and (I, ϵ) curves. Bottom: (V, I) curves for n-G/p-Si (solid line) and p-G/n-Si (dashed line) solar cells

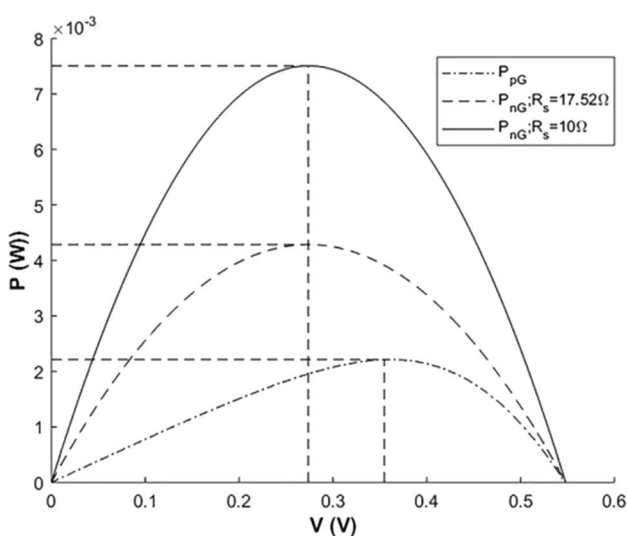


Fig. 7 (V, P) curves (p-G/n-Si, n-G/p-Si solar cell with $R_s = 17.52 \Omega$, and n-G/p-Si solar cell with $R_s = 10.00 \Omega$)

($V_{max} \approx 0.274 \text{ V}$, $I_{max} \approx 0.0157 \text{ A}$); $PCE \approx 22.55\%$, and $P_{max} \approx 0.0075 \text{ W}$ ($V_{max} \approx 0.274 \text{ V}$, $I_{max} \approx 0.0274 \text{ A}$); $PCE \approx 39.51\%$, respectively.

As we can see, the value of R_s , which depends on the solar cell's manufacturing process, is essential for obtaining solar cells with a high PCE value.

It is noteworthy that the PCE value for n-G/p-Si can exceed the value of the Shockley-Queisser limit [28]. This is because in the Shockley-Queisser limit (PCE $\approx 28\%$ for silicon PN junction-based solar cells), it has not considered the use of the current through the forward-biased diode.

To prove that actually in the n-G/p-Si solar cell there is no electric current flowing through the Schottky junction, we plotted the (V, I) curve for a diode, considering $\Phi_B = 2.94 \text{ eV}$, $R_s = 10.00 \Omega$, and neglecting a shunt resistance, as shown in Fig. 8.

Note that considering the ideality factor $\eta = 1.5$, only for voltage higher than 2.5 V, occurs a current across the diode, and for $\eta = 2.0$, only for higher voltage values than 3.5 V, occurs a current across the diode. Therefore, as the maximum voltage in the solar cell was considered 0.548 V, we can state that there is no current crossing the Schottky junction so that all photogenerated current goes to the external circuit.

Moreover, for p-G/n-Si solar cells with a small value of R_s , the external current increases (considering a fixed value of the external resistance (R)) so that the value of the external voltage also increases. Therefore, the PCE value of the solar cell p-G/n-Si increases too. However, in this case, the PCE value of this solar cell remains below the Shockley-Queisser limit.

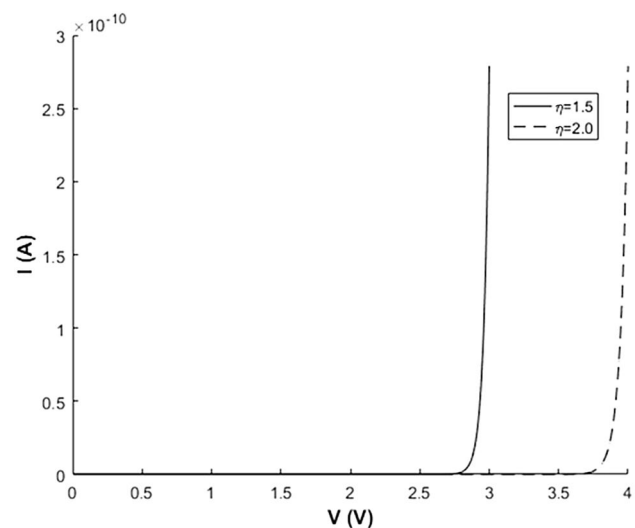


Fig. 8 (V, I) curves referring to the diode representing the Schottky junction of the solar cell p-G/n-Si (forward-bias) for $\eta = 1.5$ and $\eta = 2.0$

Since the generated photocurrent density (J_{ph}) in a solar cell is given by [29]:

$$J_{ph} = \int_{\lambda_1}^{\lambda_2} qT(\lambda)\Phi_{in}(\lambda)(1 - e^{-\alpha(\lambda)w})d\lambda, \quad (7)$$

where λ_1 and λ_2 are the minima and maximum wavelengths, that penetrate the semiconductor (UV and the semiconductor cutoffs, respectively), $T(\lambda)$ is the graphene transmittance, $\Phi_{in}(\lambda)$ is the incident photon flux, $\alpha(\lambda)$ is the optical absorption coefficient of the semiconductor and w is the width of the depletion zone, we can affirm that the type of doping and the Φ_b value do not influence the ideal generated photocurrent density.

We can further affirm that since the built-in barrier at the n-G/p-Si Schottky junction is much larger than at the p-G/n-Si Schottky junction, the number of recombinations that arise in this solar cell we are presenting should be smaller than in the p-G/n-Si solar cell. Therefore, it is expected that the n-G/p-Si solar cell has higher values of V_{oc} , I_{ph} , and PCE than those determined above (referring to the n-G/p-Si solar cell).

4 Conclusions

Currently, the maximum Schottky barrier height (SBH) for Schottky junctions composed of p-doped graphene/n-silicon is ≈ 0.8 eV. On the other hand, n-doped graphene can be obtained from metallic dopants, so that its SBH has a higher value. We presented a solar cell constituted by n-graphene/p-silicon Schottky junction, whose SBH is ≈ 2.94 eV. Due to this high SBH value, the saturated reverse current (I_0) value is very low, so that the current flowing through the Schottky junction can be neglected, which leads to an increase in the PCE value.

We showed that considering the series resistance $R_s = 17.52 \Omega$, and $R_s = 10.00 \Omega$, the PCE values are $\approx 22.55\%$, and $\approx 39.51\%$ (in this case, the PCE value is higher than the Shockley-Quiesser limit), respectively. Moreover, due to the great value of the built-in field in the n-G/p-Si solar cell we presented (which operates similarly to an electrochemical generator), the amount of recombination should be smaller than in the p-G/n-Si solar cell so that the PCE value of the n-G/p-Si solar cell can be even higher.

To show the characteristic parameters of this n-G/p-Si solar cell, we used an analytical/numerical methodology.

Funding This study was funded by Cearense Foundation for Scientific and Technological Development Support - FUNCAP (Grant Number DCR-0024-00026.03.00/15) and National Council for Scientific and Technological Development - CNPq (Grant Number 314915/2018-4).

Compliance with ethical standards

Conflict of interest The authors declare that they have no conflict of interest.

References

- Green MA, Emery K, Hishikawa Y, Warta W, Dunlop ED (2016) Solar cell efficiency tables (Version 48). Prog Photovolt Res Appl 24:905–913
- Mathew S et al (2014) Dye-sensitized solar cells with 13% efficiency achieved through the molecular engineering of porphyrin sensitizers. Nat Chem 6:242
- Yang WS et al (2017) Iodide management in formamidinium-lead-halide—based perovskite layers for efficient solar cells. Science 356:1376–1379
- Suhail A, Pan G, Jenkins D, Islam K (2018) Improved efficiency of graphene/Si Schottky junction solar cell based on back contact structure and DUV treatment. Carbon 129:520–526
- Lin Y, Li X, Xie D, Feng T, Chen Y, Song R, Tian H, Ren T, Zhong M, Wang K, Zhu H (2013) Graphene/semiconductor heterojunction solar cells with modulated antireflection and graphene work function. Energy Environ Sci 6:108–115
- Li X, Zhu H, Wang K, Cao A, Wei J, Li C, Jia Y, Li X, Wu D (2010) Graphene-on-silicon Schottky junction solar cells. Adv Mater 22:2743–2748
- Ye Y, Dai L (2012) Graphene-based Schottky junction solar cells. J Mater Chem 22:24224
- Li YF, Yang W, Tu ZQ, Liu ZC, Yang F, Zhang LQ, Hatakeyama R (2014) Schottky junction solar cells based on graphene with different numbers of layers. Appl Phys Lett 104:043903
- Meng J-H, Zhang X-W, Zhang Y, Wanga H-L, Yin Z-G, Liu H, Yan H (2016) Interface engineering for highly efficient graphene-on-silicon Schottky junction solar cells by introducing a hexagonal boron nitride interlayer. Nano Energy 28:44–50
- Cubas J, Pindado S, de Manuel C (2014) Explicit expressions for solar panel equivalent circuit parameters based on analytical formulation and the Lambert W-function. Energies 7:4098–4115
- De Blas MA, Torres JL, Prieto E, Garcia A (2002) Selecting a suitable model for characterizing photovoltaic devices. Renew Energy 25:371–380
- Saloux E, Teyssedoua A, Mikhail S (2011) Explicit model of photovoltaic panels to determine voltages and currents at the maximum power point. Sol Energy 85:713–722
- Chegaar M, Ouennoughi Z, Guechi F, Langueur H (2003) Determination of solar cells parameters under illuminated conditions. J Electron Dev 2:17–21
- Sabadus A, Mihailetchi V, Paulescu M (2017) Parameters extraction for the one-diode model of a solar cell. In: AIP conference proceedings, vol 1916, p 040005, <https://doi.org/10.1063/1.5017444>
- Adam S, Hwang EH, Galitski VM, Sarma SD (2007) A self-consistent theory for graphene transport. Proc Natl Acad Sci USA 104:18392–18397
- Victor MG, Shaffique A, Sarma SD (2007) Statistics of random voltage fluctuations and the low-density residual conductivity of graphene. Phys Rev B 76:245405
- Abhilash TS, De Alba R, Zhelev N, Craigheadb HG, Parpia JM (2015) Transfer printing of CVD graphene FETs on patterned substrates. Nanoscale 7:14109–14113
- Xia J, Chen F, Li J, Tao N (2009) Measurement of the quantum capacitance of graphene. Nat Nanotechnol 4:505–509

19. Klein C, Cohen-Elias D, Sarusi G (2018) Controlling graphene work function by doping in a MOCVD reactor. *Mater Sci Nano-technol* 4(12):e01030
20. Zhang X, Zhang L, Chan M (2016) Doping enhanced barrier lowering in graphene-silicon junctions. *Appl Phys Lett* 108:263502
21. Yang H, Heo J, Park S, Song HJ, Seo DH, Byun K-E, Kim P, Yoo IK, Chung H-J, Kim K (2012) Graphene barristor, a triode device with a gate-controlled Schottky barrier. *Science* 336:1140–1143
22. Legesse M, El Mellouhi F, Bentría ET, Madjet ME, Fisher TS, Kais S, Alharbi FH (2017) Reduced work function of graphene by metal adatoms. *Appl Surf Sci* 394:98–107
23. McCarthy PT, Van der Laan SJ, Janes DB, Fisher TS (2013) Photonically excited electron emission from modified graphitic nanopetal arrays. *J Appl Phys* 113(19):193710
24. Falkovsky LA, Pershoguba SS (2007) Optical far-infrared properties of a graphene monolayer and multilayer. *Phys Rev B* 76:153410
25. Christensen J, Manjavacas A, Thongrattanasiri S, Koppens FHL, de Abajo FJG (2012) Graphene plasmon waveguiding and hybridization in individual and paired nanoribbons. *Am Chem Soc* 6(1):431–440
26. Di Bartolomeo A (2015) Graphene Schottky diodes: an experimental review of the rectifying graphene/semiconductor heterojunction. *Phys Rep* 606:1–58. <https://doi.org/10.1016/j.physrep.2015.10.003>
27. Cheung SK, Cheung NW (1986) Extraction of Schottky diode parameters from forward current-voltage characteristics. *Appl Phys Lett* 49:85
28. Shockley W, Queisser HJ (1961) Detailed balance limit of efficiency of pn junction solar cells. *J Appl Phys* 32:510. <https://doi.org/10.1063/1.1736034>
29. Sze SM, Ng KK (2006) *Physics of semiconductor devices*, 3rd edn. Wiley, Hoboken

Publisher's Note Springer Nature remains neutral with regard to jurisdictional claims in published maps and institutional affiliations.